

Crack Initiation and Propagation Analyses of Hydrogen-Related Fracture Surfaces of Tempered Martensitic Steel



Takahiro Chiba, Takashi Yasukawa and Kenichi Takai

Abstract Hydrogen-related crack initiation and propagation in tempered martensitic steel were investigated by fracture surface topography analysis (FRASTA) and crystallographic orientation analysis. Hydrogen-related fracture morphologies of tempered martensitic steel were characterized by intergranular and quasi-cleavage transgranular fractures. FRASTA results suggested that hydrogen-related crack initiation sites were inclusions and cracks propagated from quasi-cleavage fracture to intergranular fracture near the crack initiation site. Crystallographic orientation analysis results suggested that intergranular fracture propagated on prior austenite grain boundaries, whereas quasi-cleavage fracture propagated along $\{011\}$ planes near the crack initiation site. However, quasi-cleavage fracture consisted of not only $\{011\}$ planes but also various other planes. In a previous study, hydrogen-related fracture morphologies of tempered martensitic steel tended to change from quasi-cleavage to intergranular with an increase in strength or an increase in hydrogen content, and quasi-cleavage fractures propagated along $\{011\}$ planes. However, the results of the present study indicate that the fracture propagation path changed from quasi-cleavage fracture along $\{011\}$ planes and other various planes within the prior austenite grains to intergranular fracture on the prior austenite grain boundaries caused by the influence of an inclusion.

Keywords Hydrogen embrittlement · Martensitic steel · Intergranular fracture · Quasi-cleavage fracture · Crack initiation · Crack propagation

T. Chiba (✉) · T. Yasukawa
Graduate School of Science and Technology, Sophia University, 7-1 Kioi-cho,
Chiyoda-ku, Tokyo 102-8554, Japan
e-mail: taka_rug1228@yahoo.co.jp

T. Yasukawa
e-mail: cinnaaa718@gmail.com

K. Takai
Faculty of Science and Technology, Department of Engineering and Applied Science,
Sophia University, Tokyo, Japan

© The Minerals, Metals & Materials Society 2020
The Minerals, Metals & Materials Society (ed.), *TMS 2020 149th
Annual Meeting & Exhibition Supplemental Proceedings*, The Minerals,
Metals & Materials Series, https://doi.org/10.1007/978-3-030-36296-6_126

1359

Introduction

Hydrogen enhances catastrophic and premature fracture in metals and alloys, particularly high strength steels, such as martensitic steels. This hydrogen-related fracture is termed hydrogen embrittlement. Numerous models have been proposed to account for hydrogen embrittlement fracture. To date, however, the underlying mechanism causing hydrogen embrittlement fracture is not fully understood. Thus, hydrogen embrittlement has become one of the major issues in steel research in recent years.

Martensitic steel displays two typical fracture modes in hydrogen embrittlement, intergranular and quasi-cleavage transgranular fractures. Recently, attempts to define the key to understanding the mechanism of hydrogen embrittlement. Kim and Morris observed microstructures beneath quasi-cleavage fracture surface in martensitic steels by transmission electron microscopy (TEM) and reported that hydrogen-related quasi-cleavage fracture surface was parallel to lath boundaries of martensite [1]. Based on focused ion beam machining and TEM observations, Nagao also proposed that quasi-cleavage fracture in a low-carbon martensitic steel propagated along lath boundaries [2]. Shibata investigated microstructure and crystallographic features of hydrogen-related fracture in low-carbon martensitic and ferritic steels using electron backscattering diffraction (EBSD) analysis and revealed that quasi-cleavage fracture occurred along $\{011\}$ planes [3, 4]. However, the dominant fracture surface mode has yet to be defined.

Therefore, hydrogen-related crack initiation and propagation in tempered martensitic steel were investigated in this study on the basis of fracture surface topography analysis (FRASTA) and crystallographic orientation analysis.

Experimental

Materials

Induction quenched and tempered martensitic steel was used in the present study. The chemical composition of this steel is shown in Table 1. A schematic of a specimen for the tensile test is shown in Fig. 1.

Table 1 Chemical composition of the specimens (mass%)

C	Si	Mn	P	S	Cu	Ti	B
0.30	0.21	0.72	0.019	0.002	0.01	0.03	0.002

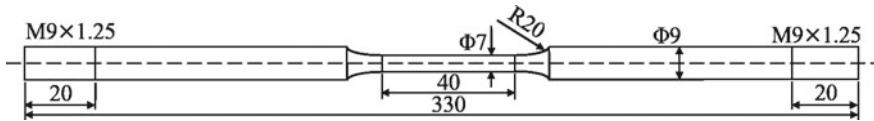


Fig. 1 Schematic of the specimen in tensile tests

Hydrogen Pre-charging, Tensile Test, and Observations

Prior to hydrogen pre-charging, the specimen surface was mechanically polished using emery papers (#800, #1000 and #2000). Specimens were cathodically charged with hydrogen in a solution of 0.1 N NaOH and 5 g L⁻¹ NH₄SCN at 30 °C and a current density of 100 A m⁻². The charging time was 96 h to reach an equilibrium hydrogen concentration both at the surface and in the center of the specimens. There charging conditions provided an equilibrium hydrogen concentration was approximately 4.5 mass ppm in the specimens. Subsequent to the pre-charging, hydrogen charging, the hydrogen-related fracture surface was obtained by conducting a tensile test at a strain rate of 0.01 mm min⁻¹ while hydrogen charging was performed under the same conditions. After tensile testing, the fracture surf of tensile-tested specimens was observed by scanning electron microscopy (SEM).

Fracture Surface Topography Analysis (FRASTA)

FRASTA is a procedure that is used to computationally reconstruct a fracture process at the microscopic level by comparing topographic features of conjugate areas in opposing fracture surfaces [5]. The procedure of FRASTA is to obtain topographic maps of conjugate areas in opposing fracture surfaces, computationally superimpose the two conjugate topographic maps until there is no gap between them, and gradually increase the relative distance between the two conjugate topographic maps. Gaps between the two conjugate topographic maps begin to appear by increasing the relative distance between them. The fracture propagation process can be reconstructed through the sequence gap formation by increasing the relative distance between the two topographic maps since it can be assumed that the gaps which appear correspond to fractured areas [6]. The sample for FRASTA was prepared using the cathodically charged and tensile-tested specimen.

Crystallographic Analysis on Hydrogen-Related Fracture Surface

Crystallographic of hydrogen-related fracture surface of the martensitic steel specimens were investigated by EBSD using the above-mentioned SEM operated at 15 kV. A trace analysis was also conducted to obtain EBSD orientation mapping and clarify the crystallographic features of hydrogen-related fracture surfaces of martensitic steel specimens. To preserve the fracture surface from corrosion, a Ni layer was electrodeposited on the hydrogen-related fracture specimen with an aqueous solution of $50 \text{ g L}^{-1} \text{ Ni}_2\text{SO}_4$, $15 \text{ g L}^{-1} \text{ NH}_4\text{Cl}$, and $15 \text{ g L}^{-1} \text{ H}_3\text{BO}_4$. One side of the electrodeposited specimen was mechanically polished, and the other side was polished with colloidal silica. The EBSD measurement and analysis were performed by using TSL OIM Data Collection and TSL OIM Analysis, respectively.

Results and Discussion

Mechanical Properties

Figure 2 shows nominal stress-strain curves of the hydrogen-uncharged specimen (black line) and the hydrogen-charged specimen (red line). The hydrogen-uncharged

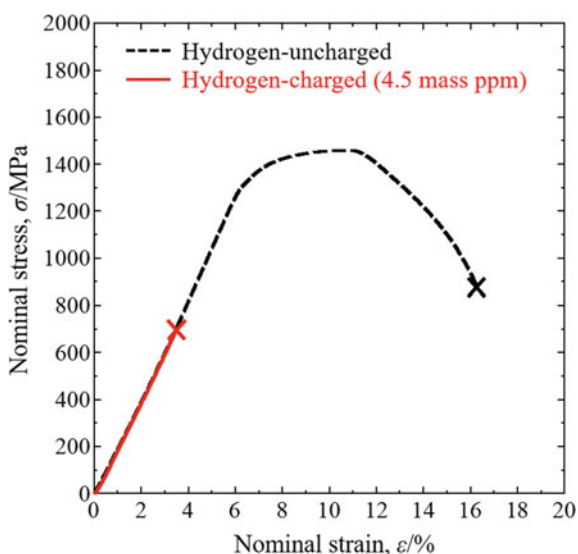


Fig. 2 Nominal stress-strain curves of hydrogen-uncharged (black line) and hydrogen-charged (red line) specimens

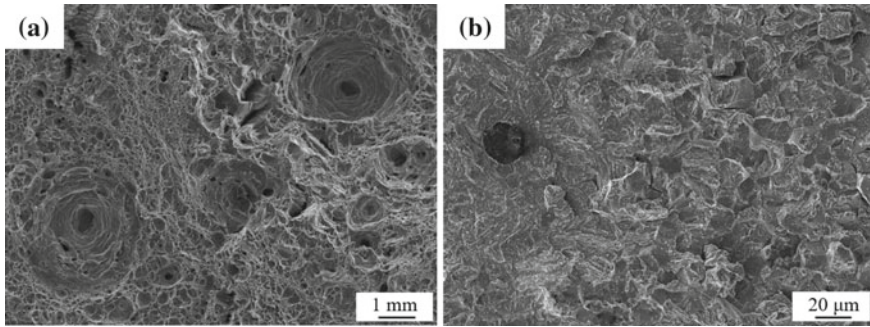


Fig. 3 SEM images of **a** hydrogen-uncharged specimen and **b** hydrogen-charged specimen

specimen fractured within the plastic region and its elongation was approximately 12.5%. In contrast, the hydrogen-charged specimen fractured within the elastic region. This result indicates that the elongation of the specimen reduced due to hydrogen charging.

Fracture Surface

SEM images of the fracture surfaces of the hydrogen-uncharged and hydrogen-charged specimens are shown in Fig. 3. The Fracture surface of the hydrogen-uncharged specimen was covered with dimple fracture (Fig. 3a). The fracture surface exhibited typical ductile fracture. In contrast, the hydrogen-charged specimen displayed quasi-cleavage and intergranular fracture surfaces. The quasi-cleavage fracture surface was observed near the inclusion and the intergranular was found a bit far away from the inclusion (Fig. 3b).

Fracture Process Reconstructed by FRASTA

Three-dimensional images of the hydrogen-charged fracture surface were obtained from three stereoscopic SEM images in Fig. 4a, b, which were taken by tilting the specimen by 0° and $\pm 5^\circ$. Mex 6.1 software was used to reconstruct three-dimensional fracture surface images. The reconstructed three-dimensional images of the conjugate fracture surfaces are presented in Fig. 4c, d. After reconstructing three-dimensional fracture surface images, the reconstructed three-dimensional image of the conjugate fracture surface was overlaid computationally until there was no gap between the two conjugate topography maps, by gradually increasing the relative distance between them. The results are shown in Fig. 5. The number (L) in the upper right corner of each figure indicates the distance between the two maps. L is defined as 0 when all areas of the two topographic maps completely overlap each other.

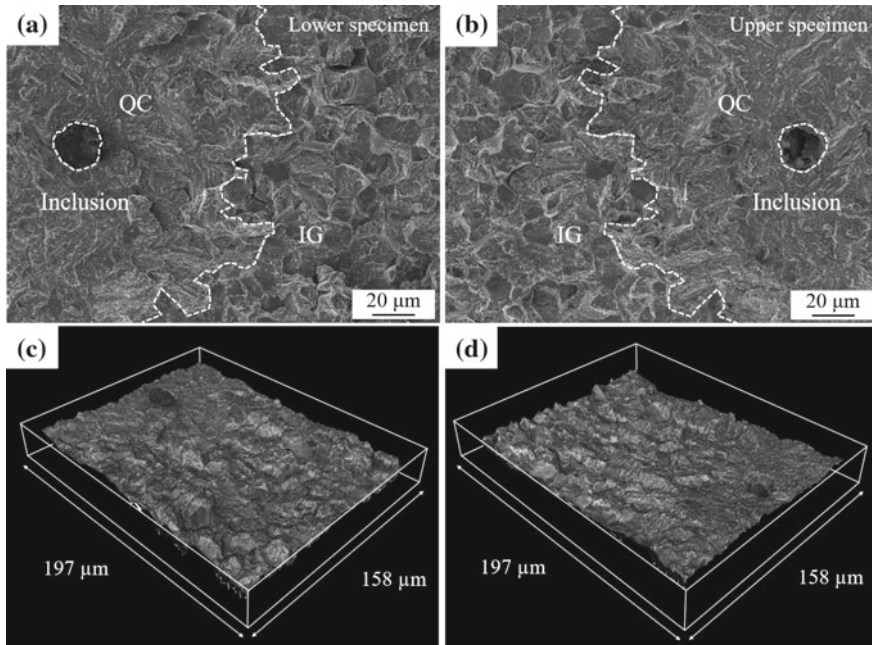


Fig. 4 SEM images of conjugate fracture surfaces of **a** lower and **b** upper specimens, and three-dimensional images of conjugate fracture surfaces of **c** lower and **d** upper specimens, respectively

In Fig. 5, fractured areas that appeared by increasing the distance between two topographic maps are represented by blue and green colors, which correspond to areas before and after crack propagation, respectively. As shown in Fig. 5a, b, it was found that the debonding of an inclusion from the surrounding matrix occurred in the early stages of hydrogen-related fracture. In the following stages of the fracture, quasi-cleavage fracture gradually propagated inside prior austenite grains. In the final stages of the fracture, intergranular fracture occurred at prior austenite grain boundaries and propagated abruptly.

Results shown in Fig. 5 indicate that hydrogen-related fracture in the martensitic steel was initiated by the inclusion. Previous studies have reported that in high carbon chromium bearing steels, the debonding of an inclusion from the surrounding matrix was promoted by hydrogen [7]. Accordingly, it is inferred that hydrogen-induced the debonding of the inclusion from the surrounding matrix. On the other hand, crack propagation occurred from quasi-cleavage fracture to intergranular fracture near the crack initiation site. In a previous study, the hydrogen-related fracture morphologies of tempered martensitic steel shifted from quasi-cleavage to intergranular with an increase in strength or hydrogen content. However, the results in Fig. 5 show that the crack propagated from quasi-cleavage fracture to intergranular fracture near the crack initiation site. Therefore, it is postulated that the fracture propagation path varied from quasi-cleavage to intergranular fracture due to the influence of the inclusion.

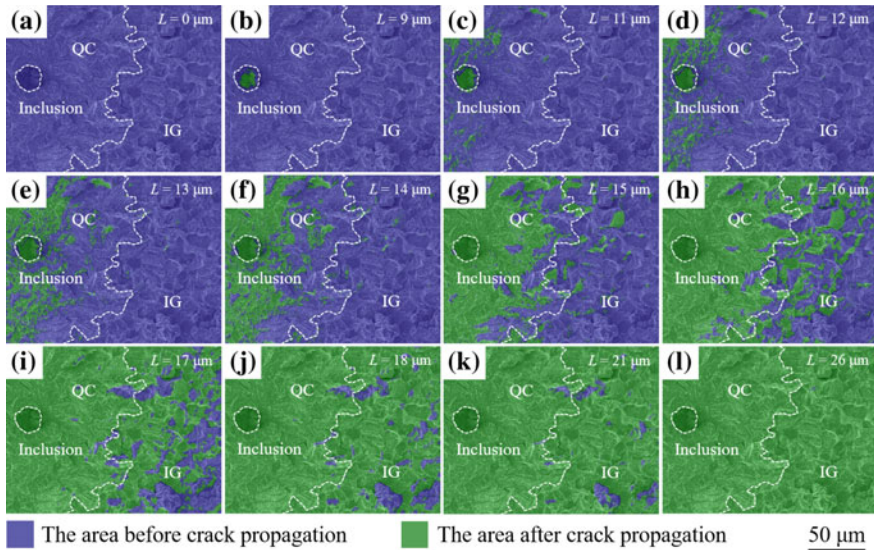


Fig. 5 Hydrogen-related fracture process reconstructed by FRASTA. Numbers (L) at the upper right corner of each figure are the distances between the two topographic maps. The fracture areas that appeared by increasing the distance between the two topographic maps are represented on the fracture surface SEM image by blue and green colors, which correspond to the areas before and after crack propagation, respectively

Crystallographic Analysis on Hydrogen-Related Fracture Surface

Figure 6a, c are SEM images and 6b, d are EBSD orientation maps of quasi-cleavage and intergranular fracture surfaces caused by hydrogen. The light gray area in the SEM images and black area in the EBSD orientation maps correspond to Ni layers. The blue line in the SEM images shows the boundary of the first surface and the red line shows the boundary of the second surface. The length of the white bar indicates the calculated translation distance value. The traces of $\{011\}$ planes showing the crystal orientation near the fracture surface displayed in yellow lines in the EBSD orientation maps. The measurement point numbers parallel to and not parallel to the $\{011\}$ planes are shown in yellow and white, respectively.

The measurement points parallel to the $\{011\}$ plane were 3/8 points of the quasi-cleavage fracture surface. Hydrogen-related fracture along $\{011\}$ planes has been reported in some martensitic steels [8, 9]. However, hydrogen-related fracture probably consists of not only $\{011\}$ slip planes but also, various crystal planes since not all points on the quasi-cleavage fracture surface are parallel to $\{011\}$ slip planes. On the other hand, the measurement points parallel to the $\{011\}$ plane were 0/8 points about the intergranular fracture surface. Presumably, cross slip occurred in the body-centered-cubic lattice owing to plastic strain induced by the inclusion on

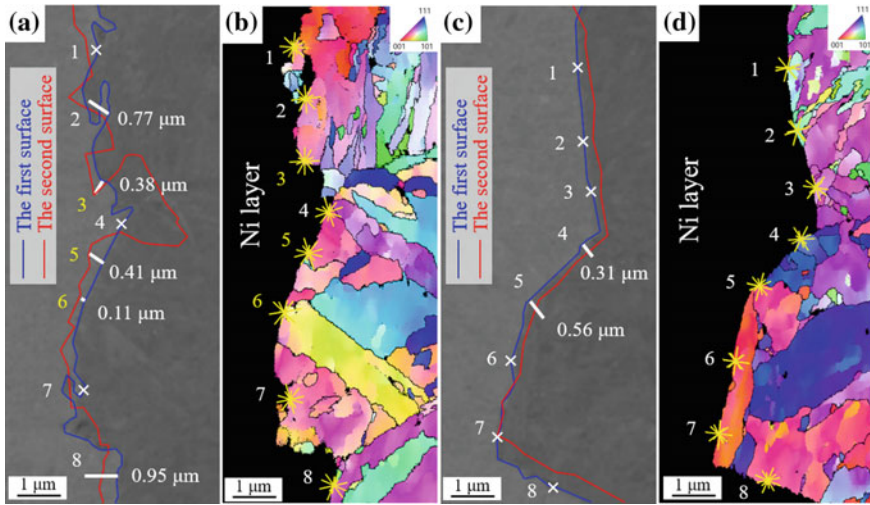


Fig. 6 Trace analyses of $\{011\}$ planes. **a** SEM image and **b** EBSD orientation map of quasi-cleavage fracture surface and **c** SEM image and **d** EBSD orientation map of intergranular fracture surface

the quasi-cleavage fracture surface and the fracture propagation path changed from quasi-cleavage fracture along $\{011\}$ planes and various other planes within the prior austenite grains to intergranular fracture on prior austenite grain boundaries due to the influence of the inclusion.

Conclusion

In the present investigation, crack initiation and propagation on hydrogen-related fracture surfaces of tempered martensitic steel were examined by crystallographic orientation analysis and FRASTA. The results that were obtained can be summarized as follows.

- (1) The hydrogen-related fracture process was reconstructed by FRASTA. In the early stages of the fracture, an inclusion was debonded from the surrounding matrix. In the following stages of the fracture, quasi-cleavage fracture gradually propagated inside prior austenite grains. In the final stages of the fracture, intergranular fracture occurred at prior austenite grain boundaries and propagated quickly.
- (2) Crystallographic orientation analyses suggested that intergranular fracture surfaces at prior austenite grain boundaries were not parallel to $\{011\}$ slip planes and that quasi-cleavage fracture surfaces propagated not only along $\{011\}$ planes but also various crystal planes.

References

1. Kim YH, Morris JW (1983) The nature of quasicleavage fracture in tempered 5.5 Ni steel after hydrogen charging. *Mater Trans A* 14:1883–1888
2. Nagao A, Smith CD, Dadfarnia M, Sofronis P, Robertson IM (2012) The role of hydrogen in hydrogen embrittlement fracture of lath martensitic steel. *Acta Mater* 60:5182–5189
3. Shibata A, Momotani Y, Murata T, Matsuoka T, Tsuboi M, Tsuji N (2017) Microstructural and crystallographic features of hydrogen-related fracture in lath martensitic steels. *Mater Sci Technol* 33:1524–1532
4. Okada K, Shibata A, Takeda Y, Tsuji N (2018) Crystallographic feature of hydrogen-related fracture in 2Mn–0.1C ferritic steel. *Int J Hydrogen Energy* 43:11298–11306
5. Kobayashi T, Shockey DA (2010) Fracture surface topography analysis (FRASTA)—development, accomplishments, and future applications. *Eng Fract Mech* 77:2370–2384
6. Shibata A, Matsuoka T, Ueno A, Tsuji N (2017) Fracture surface topography analysis of the hydrogen-related fracture propagation process in martensitic steel. *Int J Fract* 205:73–82
7. Fujita S, Matsuoka S, Murakami Y (2009) Evaluation of susceptibility to hydrogen embrittlement for vanadium added spring steel with tensile strength of 2 GPa Class. *Tetsu-to-Hagané* 95:870
8. Kim YH, Kim HJ, Morris JW (1986) The influence of precipitated austenite on hydrogen embrittlement in 5.5Ni steel. *Metall Mater Trans.* 17:1157–1164
9. Shibata A, Murata T, Takahashi H, Matsuoka T, Tsuji N (2015) Characterization of hydrogen-related fracture behavior in as-quenched low-carbon martensitic steel and tempered medium-carbon martensitic steel. *Metall Mater Trans A* 46:5685–5696